JOURNAL OF NEUROPHYSIOLOGY
Vol. 70, No. 1, July 1993. *Printed in U.S.A.*

Transient Ca^{2+} Currents in Neurons Isolated From Rat Lateral Habenula

J. R. HUGUENARD, M. J. GUTNICK, AND D. A. PRINCE
Department of Neurology and Neurological Sciences, Stanford University Medical Center, Stanford, California 94305; and Department of Physiology, Faculty of Health Sciences, Ben Gurion University of the Negev, Beersheva 84105, Israel

SUMMARY AND CONCLUSIONS

1. The properties of the low-voltage-activated transient Ca^{2+} current (LVA, I_T) that underlies rhythmic burst firing in neurons of the lateral habenula (LHb) were examined to further our understanding of mechanisms that promote rhythmogenesis in the CNS. We compared these properties with those of I_T in thalamic ventrobasal relay neurons (I_{VB}) and of the more slowly inactivating I_{Ts} of thalamic reticular neurons (I_{nRt}).

2. Patch-clamp techniques were used to record whole cell Ca^{2+} currents in LHb cells acutely isolated from rats ranging in age from postnatal days 6 to 34 (P6–P34). The LVA current in LHb (I_{LHb}) had a number of properties similar to those of I_{VB}, including activation threshold (near −65 mV) and voltage-dependent steady-state activation [half-activation voltage ($V_{1/2}$) = −58.5 mV, slope = 3.4 mV^{-1}] and inactivation ($V_{1/2}$ = −83.5 mV, slope = 5.0 mV^{-1}) functions.

3. I_{LHb} was characterized by biphasic inactivation, with a fast, voltage-dependent time constant (20–50 ms) similar to that of I_{VB} and a slower, voltage-independent decay phase (time constant ~120 ms) that was much more prominent than in I_{VB}. Recovery of I_{LHb} from inactivation was monophasic (time constant, 507 ms at −90 mV), and was slower than for I_{VB} and about the same as for I_{nRt}.

4. I_{LHb} was relatively insensitive to equimolar substitution of Ba^{2+} for Ca^{2+}, in contrast to I_{VB}, which was decreased, and I_{nRt}, which was enhanced.

5. In computer simulations, these results could not be accounted for by a mixture of the two previously described I_T types (I_{VB} and I_{nRt}) in individual LHb cells. Thus a third type of LVA current, distinct from that present in either relay neurons or reticular neurons of the thalamus, exists in LHb cells.

6. The common feature of LVA currents in highly rhythmic neurons of reticular thalamic nucleus and LHb is slow inactivation with a voltage-independent inactivation phase in both. These current properties would serve to prolong the duration of Ca^{2+}-dependent spike bursts and thereby secondarily promote rhythm generation.

INTRODUCTION

It is well established that several different types of voltage-dependent neuronal Ca^{2+} channels are present in the mammalian brain. At the most general level, these are classified according to activation-voltage relationship into high-voltage–activated (HVA) and low-voltage–activated (LVA) channels (Swandulla et al. 1991). Most studies of Ca^{2+} current diversity have focused on HVA currents, which have been variously categorized by different investigators on the basis of inactivation characteristics and pharmacological sensitivities (Tsien et al. 1991). By contrast, LVA channels and the transient currents they underlie have generally been regarded as a uniform group. However, Huguenard and Prince (1992) recently demonstrated that differences in LVA currents also exist. Using whole-cell voltage-clamp recordings from isolated thalamic neurons, they showed that the properties of LVA currents in the GABAergic neurons of nucleus reticularis (nRt) are clearly different from those of the thalamocortical relay neurons of nucleus ventralis basalis (VB). The LVA current of nRt cells has been termed "I_{Ts}" because it has significantly slower kinetics of activation, inactivation, and recovery from inactivation than I_T of VB cells. In addition, I_{Ts} is markedly enhanced when Ba^{2+} is substituted for Ca^{2+}, whereas the I_T of VB neurons is generally suppressed in Ba^{2+}. It was suggested that these differences in I_T characteristics may underlie observed differences in rhythmic voltage activities of VB versus nRT neurons (Huguenard and Prince, 1992). In both cell types, recovery from inactivation (deinactivation) of the LVA current is a critical step in the production of a rebound spike burst after a brief hyperpolarization; however, rebound bursts are more prolonged in the GABAergic nRt cells (Avanzini et al. 1989; Huguenard and Prince 1992; Llinás and Geijo-Barrientos 1988; Mulle et al. 1986).

In vivo studies have implicated nRt neurons as the pacemakers for thalamocortical rhythms on the basis of their electrophysiological activities (Mulle et al. 1985; Steriade et al. 1985, 1987), whereas widespread intrathalamic connections (Jones 1985) provide an anatomic basis for such pacemaking. Intracellular studies in thalamic slices indicate that subtle alterations in membrane potential of nRT cells, such as those induced by serotonin or noradrenaline (McCormick and Wang 1991), can evoke prolonged periods of sustained rhythmicity, with membrane potential continuously oscillating between rebound bursts and subsequent hyperpolarizations. Similar manipulations in neurons of many relay nuclei in the rat and guinea pig generally evoke either a single burst or a brief oscillatory epoch that is rapidly damped, exceptions being neurons of the dorsal lateral geniculate (Leresche et al. 1990; Pape and McCormick 1989) and paratenial (McCormick and Prince 1988) nuclei.

The present study was undertaken to further explore the diversity of LVA current types. If functional differences in oscillatory behavior are related to underlying differences in I_T, we reasoned that I_{Ts} might predominate in neurons of other brain regions whose oscillatory activities are similar to those of nRt. We therefore examined the properties of the LVA current in neurons isolated from the lateral habenula (LHb), a rhythmogenic subthalamic nucleus whose af-

ferent and efferent connections constitute an important pathway through which forebrain structures influence neuronal activities in the midbrain. In an intracellular study in slices, Wilcox et al. (1988) showed that LHb neurons resemble nRt neurons in that they produce a very pronounced rebound burst after a single, brief hyperpolarizing stimulus, and they have a marked tendency to continuously oscillate for long periods during which they rhythmically generate low-threshold Ca^{2+} spikes. We now report that, despite this similarity of behavior in voltage recordings, the characteristics of LVA current in LHb neurons are different from those of neurons in both VB and nRt in terms of kinetics of activation and inactivation and current amplitude with Ba^{2+} as the charge carrier. These differences seem to place the LHb I_T properties midway between those of VB and nRt. The data are consistent with the view that there are a variety of LVA currents in the brain that reflect a diversity of underlying Ca^{2+} channel types. These results have been published in preliminary form (Huguenard et al. 1992).

METHODS

Cell preparation

Acutely isolated LHb cells were obtained using previously described techniques (Huguenard and Prince, 1992). Rats of either sex, postnatal age 6 to 34 days (P6–P34), were anesthetized (pentobarbital sodium 50 mg/kg) and decapitated. The brain was rapidly removed, blocked with a scalpel cut in the parasagittal plane, and glued with the lateral face down; 500-μm parasagittal slices were cut with a vibratome (TPI, St. Louis, MO). Of the three most medial slices, the center one usually contained medial habenula and portions of LHb, whereas the two immediately adjacent slices contained the major portions of the left and right LHb, which extended throughout the slices (Fig. 1). Slices containing the LHb were readily identified because fasciculus retroflexus (fr) could be observed on both the medial and lateral surfaces of the slice. Slices were washed, incubated for 30–60 min in an enzymatic mixture [3 mg/ml protease type XXIII (Sigma) and 2.5 mg/ml collagenase (Worthington) in piperazine-*N,N'*-bis(2-ethanesulfonic acid) (PIPES)-buffered saline; see below], and washed again. Each LHb was subdissected from its slice, and then triturated in PIPES saline. A yield of 10–20 viable neurons per animal was achieved.

Solutions

The PIPES-buffered saline used in the preincubation and incubation steps consisted of (in mM): 120 NaCl, 5 KCl, 1 $MgCl_2$, 1 $CaCl_2$, 25 glucose, and 20 PIPES, and the pH was adjusted to 7.0 with NaOH (Kay and Wong 1986). Calcium currents were recorded with the whole cell patch recording technique (Hamill et al. 1981) using the following solutions (in mM): pipette solution —110 tris(hydroxymethyl)aminomethane (Tris) PO_4 dibasic 28 Tris base, 11 ethylene glycol-bis(β-aminoethyl ether)-*N,N,N',N'*-tetraacetic acid (EGTA), 2 $MgCl_2$, 0.5 $CaCl_2$, 4 Na_2 ATP, 22 phosphocreatine, and 50 U/ml creatinine phosphokinase, pH 7.3; extracellular solution—155 tetraethylammonium-Cl, 3 $CaCl_2$, 10 *N*-2-hydroxyethylpiperazine-*N'*-2-ethanesulfonic acid (HEPES), pH 7.4. In some experiments additional measures were taken to reduce contamination of T currents by HVA currents; either CsF was substituted for Tris-PO_4 as the primary intracellular electrolyte (Carbone and Lux 1987), or ATP and the creatinine phosphate system (Forscher and Oxford 1985) were omitted from the intracellular fill to promote HVA rundown. These manipulations had no substantive effects on the parameters of T current measured here.

Recordings

Patch-clamp electrodes were formed in two stages from borosilicate glass (KG-33 I.D. 1.0, O.D. 1.5 mm; Garner Glass, Claremont, CA) using a Narishige pp-83 electrode puller. Electrode resistance was ~4 MΩ in the bath and ranged from 7 to 12 MΩ during whole cell recording. Series resistance compensation (normally 70%) was regularly employed using the built-in circuitry of a List EPC-7 patch clamp amplifier. Because calcium currents in LHb cells were normally smaller than 300 pA, even the worst-case series resistance error would be small (<1 mV). Leak and capacitative currents were subtracted with a P/−4 procedure (Coulter et al. 1989). Cell capacitance was determined by integrating the current step obtained in response to a small voltage step, and then dividing the resultant charge (in fC) by the voltage step (in mV) to obtain capacitance (in pF). To study pharmacological effects, we made rapid extracellular solution changes with a multibarrel perfusion system that was brought close to the cell under visual control. All effects were reversible upon wash.

Protocols and analysis

Ca^{2+} current separation was performed as in previous studies. To examine the pharmacological effects of Ca^{2+} agonists and antagonists, isolated T current was activated by stepping the membrane potential from −100 to −40 mV, and HVA current was activated by stepping from −40 to 0 mV. Because T currents inactivate completely (Carbone and Lux 1987; Coulter et al. 1989; Fox et al. 1987; Huguenard and Prince 1992), for this study they were measured as the "inactivating current," which was obtained by subtracting the steady-state current from the peak current at each command potential. The results of LHb cell recordings reported here were compared with those obtained in a previous study of VB and nRt cells performed under the same conditions (Huguenard and Prince 1992). Also, some VB cells were obtained in the same animals as those from which LHb neurons had been isolated. The results of recordings from 26 LHb neurons and 4 VB neurons are presented here. For descriptive purposes, in this paper we will refer to the T currents in the various cell types as I_{VB}, I_{nRt}, and I_{LHb}. Although there are two forms of T current in nRt cells (Huguenard and Prince 1992), in this context I_{nRt} refers to the slowly inactivating current (I_{Ts}). Activation and inactivation kinetics were obtained by fitting curves (Eq. 1, below) to experimental data. Equation 1 is based on Eq. 19 of Hodgkin and Huxley (1952), and therefore makes the same assumptions [i.e., that resting activation is small ($m_o \sim 0$ at V_H of −100 mV; see Fig. 4*C*) and that inactivation is nearly complete (i.e., $H_\infty \sim 0$ for V_C greater than −60 mV)]. These conditions apply for estimation of τ_m in Fig. 3*B* (filled symbols). We make the additional assumption that a common activation process underlies both inactivation components of I_{LHb}.

RESULTS

Ca^{2+} currents in LHb cells

Several notable distinctions exist between I_{nRt} and I_{VB} (Huguenard and Prince 1992), including differences in amplitude, steady-state activation, kinetics of inactivation and activation, and current amplitude with Ba^{2+}. We examined these properties for I_{LHb} to determine whether it resembled I_{nRt}, as hypothesized.

Initially, we compared current amplitudes by using current-voltage (*I-V*) curves (Fig. 2). In LHb cells, transient currents obtained with small depolarizations had a

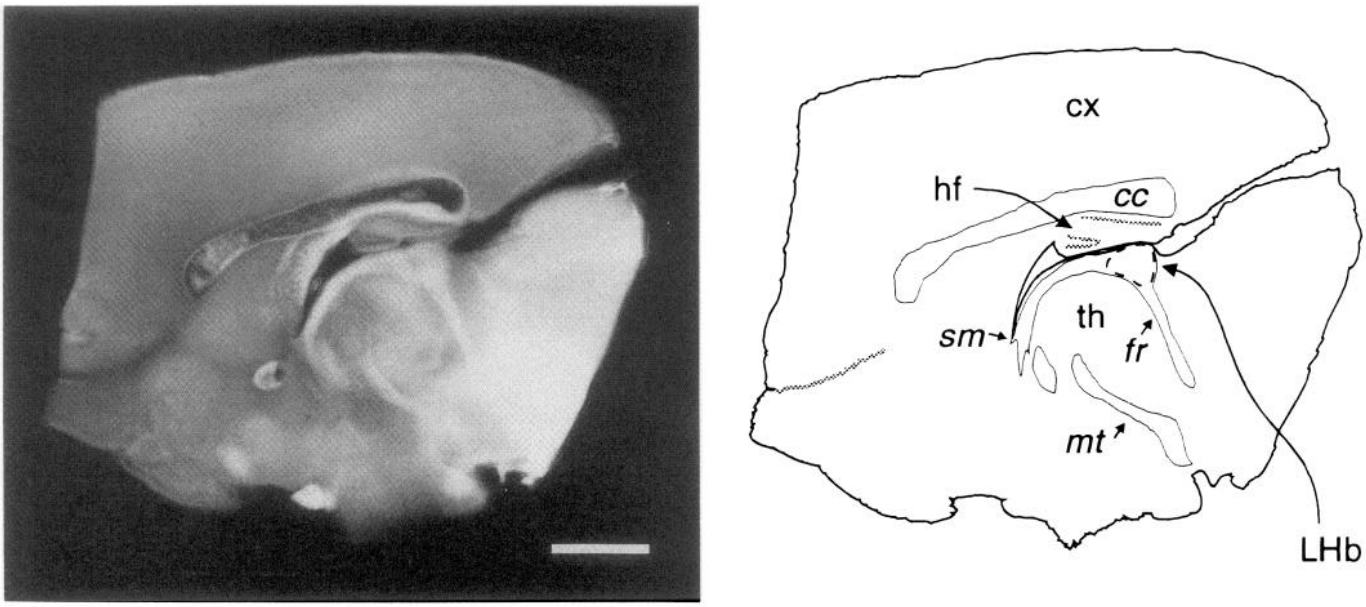

FIG. 1. Identification and isolation of lateral habenular nucleus (LHb). *Left*: a typical parasagittal slice containing LHb, cut ~500 μm from midline. LHb is easily identified at intersection of 2 major white matter tracts, stria medularis (sm) and fasciculus retroflexus (fr). Knife cuts indicated by dashed lines (*right*) are used to completely isolate LHb. cx, cortex; hf, hippocampal formation; mt, mammilothalamic tract; th, thalamus; cc, corpus callosum.

number of features similar to those in VB cells. When hyperpolarized holding potentials were used (more negative than −70 mV), depolarizations to −60 mV activated currents that were small, slowly activating, and slowly inactivating (Fig. 2, *top left*). Currents evoked by further depolarization were larger and had more rapid activation and inactivation kinetics. Although inactivation was complete in <400 ms, significant residual current was recorded at 150 ms in LHb and nRt neurons, but not in VB neurons (compare currents at open arrows in the representative cell from each structure in Fig. 2). In general, Ca^{2+} currents in LHb cells were small, averaging 140 pA at −40 mV (see *I-V* relationships in Fig. 2, *inset*). As with I_{VB}, the apparent activation threshold of I_{LHb} was −65 mV, and maximum current occurred at −35 to −40 mV. By contrast, activation threshold for I_{nRt} was positive to −60 mV and maximum current (220 pA) occurred near −30 mV (Fig. 2, *inset;* see also Huguenard and Prince 1992).

The differences in peak amplitudes of I_{LHb} and I_{VB} could not be completely accounted for by differences in cell size. Although LHb cells were smaller (10.1 ± 0.85 pF, $n = 26$) than isolated VB or nRt cells (16.7 and 17.1 pF, respectively; Huguenard and Prince 1992), this 70% difference in membrane area was not sufficient to account for the greater than threefold difference in maximum current amplitude between VB and LHb cells shown in the *I-V* plots of Fig. 2, *right*. Thus, although the *I-V* relationship of I_{LHb} is qualitatively similar to that of I_{VB}, normalizing for membrane area reveals that the current density is smaller in LHb cells. Current amplitude was not related to postnatal age, nor was it correlated with cell size, as measured by whole cell membrane capacitance.

Activation kinetics of I_{LHb}

The activation rate of I_{VB} was faster than that of I_{nRt}; as a consequence, currents in VB cells had a shorter time to peak (Huguenard and Prince 1992). Activation kinetics of I_{LHb} were intermediate between those of the two previously described currents. In general, I_{LHb} attained peak later than I_{VB} (Fig. 3*A*); thus, in 7 out of 12 LHb cells times to peak were greater than the average time to peak for VB cells (– – – in Fig. 3*A*), yet were much smaller than the average time to peak for nRt cells (--- in Fig. 3*A*). The remaining five LHb cells were similar to the average VB cell in terms of time to peak. As an internal control for possible day-to-day variability in experimental conditions, in several experiments we also compared time-to-peak T current in sample VB neurons isolated from the same brains as those used to obtain LHb cells. Measurements for one such cell are shown in Fig. 3*A* (◈); the times to peak in this VB neuron were shorter at all voltages than those of all LHb cells we studied.

The time constant of activation (τ_m) was determined by fitting Hodgkin-Huxley (1952) curves to the current traces using the m^2h formalism (Huguenard and Prince 1992; see Eq. 1 below). The values thus obtained were used to construct the right half of the bell-shaped curve relating τ_m to voltage (Fig. 3*B*, filled circles). Points on the curve to the left of the peak (Fig. 3*B*, open circles) were obtained from the deactivation rate, as described by Huguenard and Prince (1992). Figure 3*B* shows that, in the voltage range most pertinent to activation, between −55 and −35 mV, values of τ_m in LHb cells fell midway between those of nRt (---) and those of VB (– – –).

The activation curve of I_{LHb} (Fig. 4, *A* and *C*) was determined by using a tail current protocol (Huguenard and Prince 1992) and found to be similar to that of I_{VB}. The half-activation point was −58.2 ± 2.8 mV, $n = 5$, and the slope was 3.4 ± 0.5 mV^{-1}. These values compare well with those published (Huguenard and Prince 1992) for I_{VB} (−59 ± 1.7 mV and 5.2 ± 0.5 mV^{-1}), but differ from those for I_{nRt} [−50 ± 2.3 mV ($P < 0.05$) and 7.4 ± 1.1 mV^{-1}].

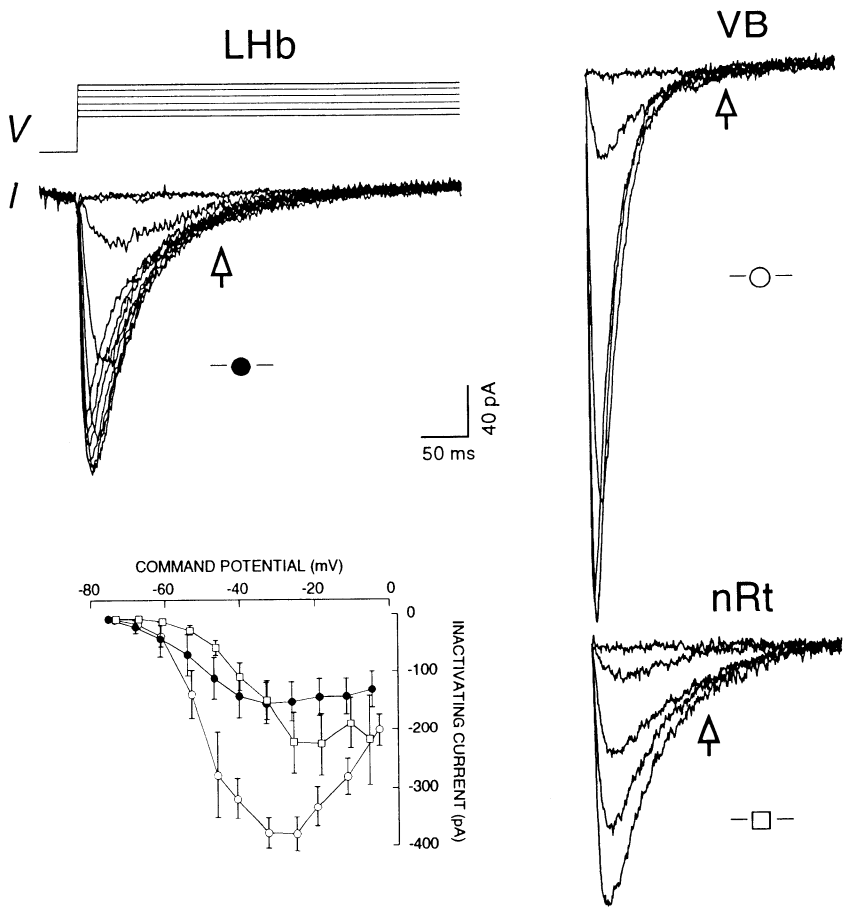

FIG. 2. Transient Ca^{2+} currents in LHb cells compared with those in nucleus ventralis basalis (VB) and nucleus reticularis (nRt). *Top left*: inward currents recorded from an isolated LHb P34 cell. To promote washout of high-voltage-activated (HVA) currents, ATP and creatinine phosphate were omitted from the intracellular fill (Forscher and Oxford 1985). *Top traces*: voltage-clamp protocol; *bottom traces*: resultant whole-cell clamp currents. Voltage steps were from a holding potential of −100 mV and spanned range from −68 to +2 mV. Inward (downward) currents became larger and peaked earlier as depolarization was increased to −40 mV, and then decreased in amplitude with further depolarization. Ca^{2+} current has not completely activated at latency of 150 ms (⇑), but inactivation is essentially complete at a latency of 400 ms. To isolate transient Ca^{2+} currents, we subtracted HVA currents activated by voltage steps from a holding potential of −40 mV from currents obtained with a holding potential of −100 mV (Huguenard and Prince 1992). *Top right*: example traces of I_{VB}. Currents activate and inactivate in a voltage-dependent manner similar to that for I_{LHb}; however, I_{VB} is larger, and completely inactivates within 150 ms (⇑). *Bottom right*: example traces of I_{nRt}. Rate of activation and inactivation is relatively independent of voltage, and currents are smaller than I_{VB} traces. Significant current remains 150 ms after onset of depolarization. *Inset*: comparison of current-voltage relationships for inactivating component of Ca current as defined in METHODS for LHb, VB, and nRt neurons. VB cells (○, n = 9, from a previous study) had an activation detection threshold near −65 mV, and largest peak currents with maximum averaging near 400 pA at −35 mV. LHb cells (●, n = 14) had a similar activation voltage but smaller peak currents with a maximum of ~150 pA near −35 mV. Cells from nRt (□, n = 9, also from a previous study), on the other hand, had a higher activation threshold (more positive than −60 mV), and had peak currents around 200 pA at −30 mV. Error bars are SE in this and subsequent figures.

Inactivation of I_{LHb}

Although differences in the kinetics of activation of I_{LHb} and I_{VB} were subtle, there were prominent distinguishing features in the decay phase of the current. As can be seen in the superimposed traces of Fig. 5*A*, relaxation of I_{LHb} clearly consisted of a slow as well as a fast inactivation component. Therefore two exponentials were necessary to fit

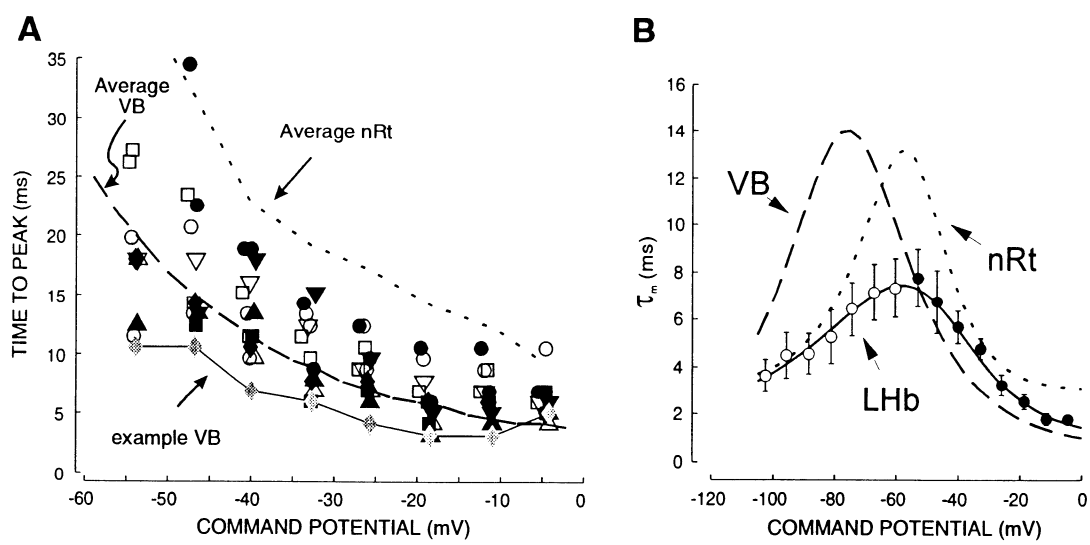

FIG. 3. Comparison of activation rates between I_{VB}, I_{nRt}, and I_{LHb}. *A*: time to peak as a function of membrane potential. Each open or black symbol represents data from a single LHB cell. Most LHb cells had times to peak between those of average nRt and average VB cell (both averages are derived from data of a previous study). All LHb cells had longer times to peak than those of a VB cell (◈) isolated with LHB cells for this study. *B*: voltage dependence for activation time constant (τ_m) in LHb cells compared with average curves for VB (– – –) and nRt (---; Huguenard and Prince 1992). Filled symbols obtained from fitting Eq. 1 to current traces, whereas open circles are twice deactivation time constant.

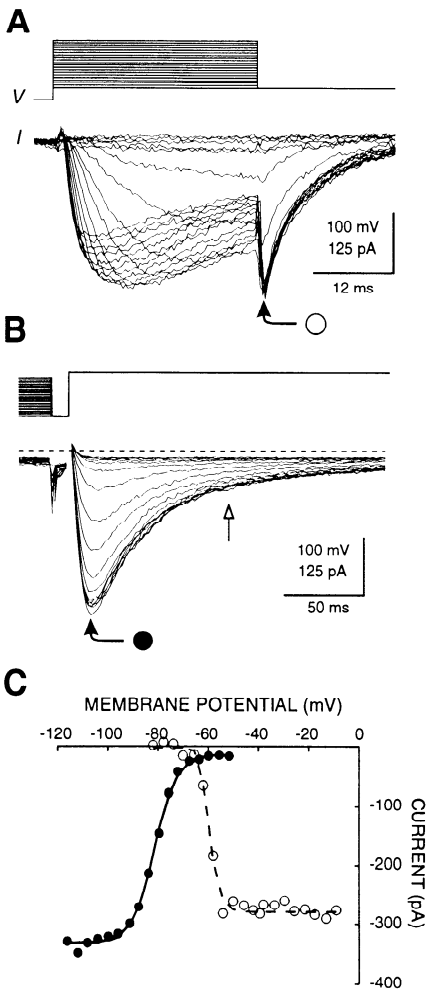

FIG. 4. Activation and steady-state inactivation properties of I_{LHb}. *A*: tail-current activation protocol for I_{LHb}, in which currents were evoked by 30-ms depolarizing steps (range −82 to −9 mV) from a holding potential of 100 mV. At completion of depolarizing step, membrane potential was stepped to −80 mV and tail-current amplitudes were measured at a latency of 1 ms. These were plotted as a function of the depolarizing command (○) in *C*. *B*: steady-state inactivation protocol, in which 1-s conditioning pulses (range −116 to −51 mV) were applied before a brief (10 ms) step to −116 mV, that preceded a test step to −40 mV. Leak currents were not subtracted. Peak currents (●) are plotted in *C* as a function of conditioning voltage. Current amplitude at a latency of 100 ms from onset of test pulse (⇑) was dependent on conditioning potential in much the same way as peak current. *C*: experimental data from *A* and *B*, with fitted Boltzmann curves. For activation, parameters were $V_{1/2} = -61.6$ mV, $k = -2.3$ mV^{-1}, $R = 0.992$, power factor = 2; for steady-state inactivation of peak currents (●), $V_{1/2} = -81.4$ mV, $k = 4.4$ mV^{-1}, $R = 0.999$, power factor = 1. Corresponding values for currents at 100-ms latency (not shown) are $V_{1/2} = -79.3$ mV, $k = 5.5$ mV^{-1}, $R = 0.996$, power factor = 1.

the decay of I_{LHb}, as follows, on the basis of Hodgkin and Huxley (1952)

$$I_{LHb} = [1 - \exp(-\frac{t}{\tau_m})]^2 \times [a1 \times \exp(-\frac{t}{\tau_{h1}}) + a2 \times \exp(-\frac{t}{\tau_{h2}})] \quad (1)$$

where $a1$ and $a2$ are coefficients for the two decay components (with units of picoamperes). I_{VB} inactivation, on the other hand, can be accurately fitted with a single decay component (Coulter et al. 1989; Huguenard and Prince 1992). Nevertheless, to facilitate direct comparison of the inactivation time course in the two cell types, we reanalyzed the I_{VB} data by fitting traces to Eq. 1. For the example in Fig. 5*A*, the relative weight of the fast inactivation component was 89% in the VB neuron, but only 71% in the LHb cell.

Figure 4*C*, which summarizes the data for all the recordings, shows that the greater prominence of the slow component of the inactivation time course was a general feature of I_{LHb} compared with I_{VB}, especially in the voltage range of −50 to −30 mV. Figure 5*B* shows that the fast and slow time constants of inactivation were not different for these two cell types. Interestingly, absolute values of $a2$ were also similar for the two cell types (not shown). Hence, the differences in relative weight reflect a higher absolute value for the fast component in VB neurons. Attempts to detect a fast component of inactivation in nRt cells always yielded negligible values; slow time constants are shown in Fig. 5*B* for comparison. For I_{VB} the relative contribution of $a1$ became progressively smaller with command potentials positive to −25 mV (Fig. 5*C*). This was probably due to slow inactivation of HVA components because those recordings of I_{VB} were obtained under conditions that maximize by inhibiting rundown (Coulter et al. 1990; Forscher and Oxford 1985; Huguenard and Prince 1992).

Steady-state inactivation values for peak I_{LHb} (Fig. 4*B*, half-inactivated potential −83.5 ± 1.2 mV, $n = 14$) were essentially the same as those for peak I_{VB} (−81 ± 1.2 mV; see Huguenard and Prince 1992). Moreover, the slope of the inactivation function was not different for the two cell types (5.0 ± 1.2 mV^{-1} for LHb vs. 4.4 ± 0.2 mV^{-1} for VB in the previous study). Steady-state inactivation properties for I_{LHb}, when measured at 100 ms after the onset of the depolarizing step (⇑ in Fig. 4*B*), yielded values for half-inactivated voltage (84.1 ± 2.8 mV, $n = 10$) and slope (−4.3 ± 0.8 mV^{-1}) that were not different from values measured at the time of the peak currents.

The time course of recovery of I_{LHb} from inactivation was much slower than that of I_{VB}. As shown in Fig. 6, recovery was quantified by holding the membrane at −40 mV, systematically increasing the durations of hyperpolarizing steps to −90 mV, and measuring the consequent peak currents on return to −40 mV. The resultant curves were well fitted with a single exponential, as in Fig. 6*B*. Time constants of recovery were 507 ± 30 ms ($n = 7$) for I_{LHb}, 298 ± 23 ms ($n = 8$) for I_{VB}, and 577 ± 22 ms ($n = 8$) for I_{nRt}. As can be seen from the histogram of Fig. 6*C*, recovery of I_{LHb} was much more similar to that of I_{nRt} than to I_{VB}.

Sensitivity of I_{LHb} to divalent cations and drugs

As previously reported (Huguenard and Prince 1992), one of the major differences between I_{VB} and I_{nRt} is the relative current amplitude when Ba^{2+} was substituted for extracellular Ca^{2+} as a charge carrier. In contrast to a 66% reduction in peak amplitude of I_{VB} when extracellular Ca^{2+} was replaced by Ba^{2+}, the same manipulation resulted in a marked increase in I_{nRt} to 150% of control. As illustrated in the examples of Fig. 7*A*, the effects of Ba^{2+} on I_{LHb} were intermediate between these extremes. On average, Ba^{2+} substitution had little or no effect on peak I_{LHb} at −40 mV (92 ± 4% of control, $n = 18$); however, Ba^{2+} did alter the time course of I_{LHb}. In the example of Fig. 7, Ba^{2+} current had a slightly increased peak amplitude and a more prominent slow decay component.

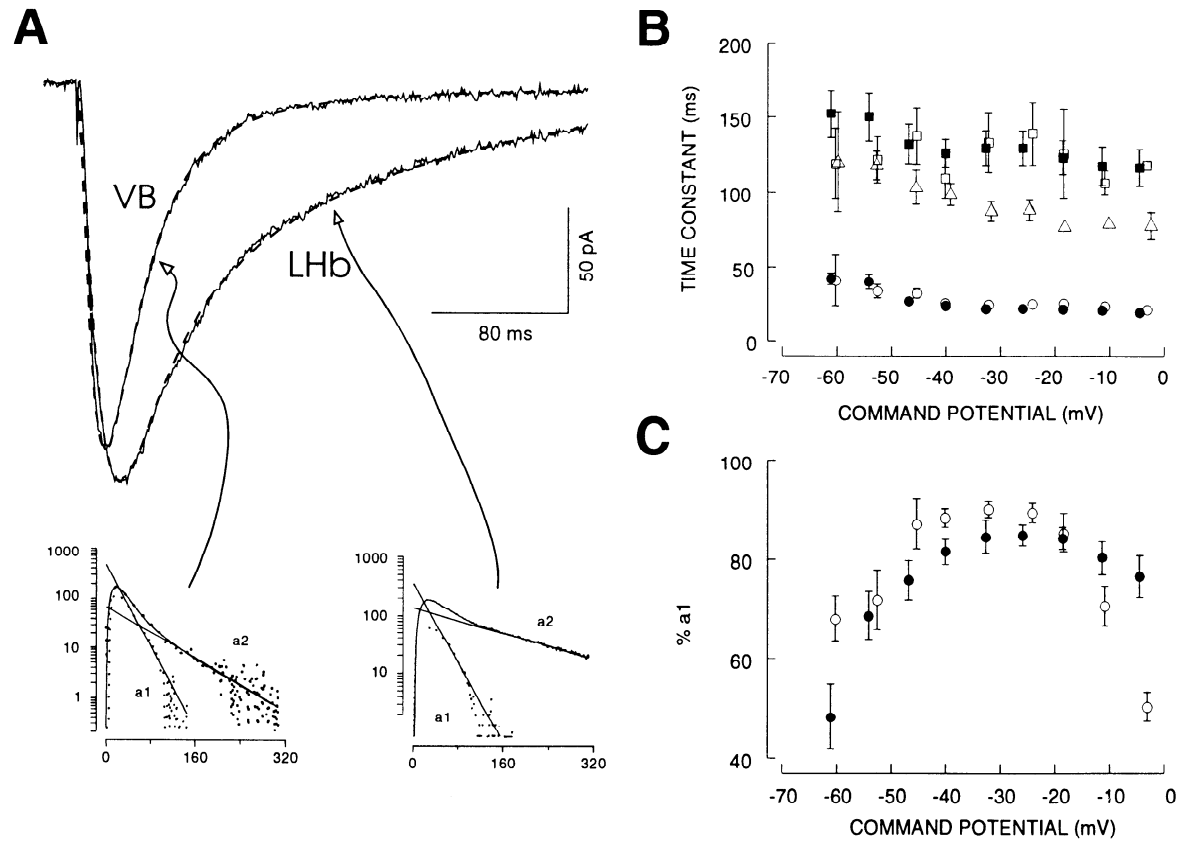

FIG. 5. I_{LHb} inactivation kinetics. *A*: fitted curves [Eq. 1, after Hodgkin and Huxley (1952), dashed lines] to current traces from typical VB and LHb cells obtained in this study. These cells had approximately the same LVA current amplitude at −40 mV. Inactivation was fit in each case as sum of 2 exponential components. *Bottom traces* contain semilog plots of current traces (dotted lines) along with fitted curves (solid lines). The 2 straight lines on each plot represent the 2 decay components, and extrapolated zero time amplitude (at *left end* of lines) are the 2 coefficients, $a1$ and $a2$. For this VB cell $a1$ = 480 pA and $a2$ = 61 pA (89% $a1$), τ_1 = 20 ms, τ_2 = 65 ms, and τ_m = 9.8 ms. For LHb cell $a1$ = 360 pA and $a2$ = 150 pA (71% $a1$), τ_1 = 24 ms, τ_2 = 140 ms, and τ_m = 12.6 ms. *B*: inactivation time constants for slow (■, LHb, n = 8; □, VB, n = 8; △, nRt, n = 7) and fast (●, LHb; ○, VB) inactivation components. *C*: relative contribution of fast decay component as a function of voltage in LHb (●, n = 8) and VB (○, n = 8). Values were calculated as $\%a1 = a1 \cdot 100/(a1 + a2)$, where $a1$ and $a2$ are coefficients of fast and slow decay components, respectively.

Although not examined in detail, when tested, the pharmacological sensitivity of I_{LHb} was found to be similar to that of I_{VB} and I_{nRt}. Cd^{2+} (0.05–0.5 mM) caused concentration-dependent reductions in I_{LHb} (Fig. 7*B*, 25–73%, n = 4). This is comparable to the 39 and 35% reduction in I_{nRt} and I_{VB}, respectively, by 0.2 mM Cd^{2+} (Huguenard and Prince 1992). The reduction by Cd^{2+} was uniform throughout the time course of I_{LHb} (Fig. 7*B*), indicating that both rapidly and slowly inactivating components have similar sensitivities. This shows that there was little or no contamination of I_{LHb} by inactivating HVA components, because the latter are very sensitive to Cd^{2+} blockade (Fox et al. 1987; Huguenard and Prince 1992). I_{LHb} amplitude was reduced by the anticonvulsant methylphenylsuccinimide (1 mM, 30% reduction, n = 2) to a similar extent as I_{VB} (Coulter et al. 1990). Finally, I_{LHb} was almost completely blocked (1 mM, 95% reduction, n = 2) by the dimethyl derivative of amiloride (Tang et al. 1988).

DISCUSSION

Previous work in this laboratory demonstrated that the kinetic and voltage-dependent properties of I_{nRt} are distinct from those of I_{VB} (Huguenard and Prince 1992). In the present study, we have examined I_{LHb} under the same experimental conditions and determined that it is not identical with either of these thalamic LVA currents, although it is in some ways similar to each of them. For example, the voltage activation range of I_{LHb} was the same as that of I_{VB}. Also, inactivation time constants were the same for both currents when two exponentials were used to fit I_{VB}, although decay of I_{VB} can generally be well fitted by a single exponential, whereas decay of I_{LHb} always follows two clear inactivation phases. The microscopic processes underlying macroscopic current inactivation are likely to be complex. For example, Aldrich et al. (1983) have shown that Na^+ current inactivation is actually the consequence of the activation process, and that inactivation of single Na^+ channels is not a voltage-dependent process. Thus single-channel studies (e.g., Chen and Hess 1990) will be necessary to fully characterize the voltage-dependent gating properties of I_{LHb} and I_{nRt}. Nevertheless, for the purposes of this study, the main conclusion is that I_{LHb} exhibits prominent biexponential decay that is much less obvious in I_{nRt} and I_{VB}.

One clear difference between I_{LHb} and I_{VB} was the consistently larger contribution of the slow inactivation component to I_{LHb} in the functionally critical voltage range of −50 to −25 mV. Activation kinetics were also generally slower

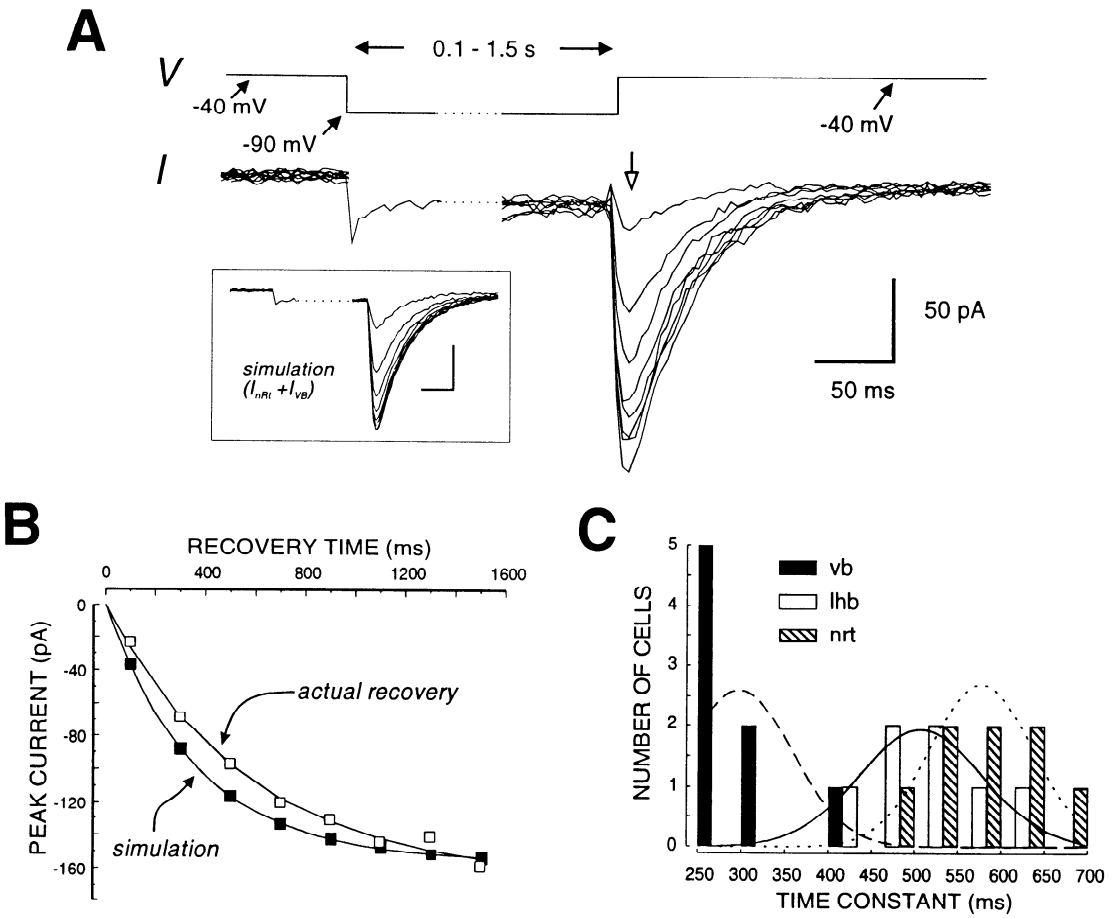

FIG. 6. Recovery of I_{LHb} from inactivation. *A*: recovery protocol. Holding potential was −40 mV, and variable duration conditioning pulses to −90 mV were applied every 5 s. With brief hyperpolarizations recovery of I_{LHb} was minor (a 100-ms conditioning pulse produced smallest current at ⇓), and current amplitude increased in an exponential manner as hyperpolarization duration was increased. *Inset*: simulation of recovery from inactivation (same protocol as in Fig. 5) for a composite current made up of 33% I_{nRt} and 67% I_{VB}. Gaussian noise with an SD of 1 pA was added to simulated currents so fitted curves obtained by nonlinear least-squares fitting routines would be subjected to same error as experimental data. *B*: peak current amplitude (□) as a function of recovery time. Solid curve is best fitted exponential with a time constant (τ) of 570 ms. Simulation data (■) could be fitted with a single exponential that had a time constant of 360 ms. *C*: recovery time constants in 3 neuronal types at a potential of −90 mV. I_{VB} was fastest to recover (average τ of 298 ms), whereas I_{LHb} was slower (τ = 507 ms), and I_{nRt} was slowest (τ = 577 ms).

for I_{LHb} than for I_{VB}. Here too, the difference was particularly clear at −50 to −25 mV, where the activation time constant of I_{LHb} fell midway between those of I_{VB} and the slower I_{nRt}. Time course of recovery of I_{LHb} from inactivation was the same as that of I_{nRt} and very much slower than that of I_{VB}. There were also pronounced differences in relative current size with Ca^{2+} or Ba^{2+}. When Ba^{2+} is substituted for Ca^{2+}, I_{VB} decreases by ~40%, whereas I_{nRt} increases by 50% (Huguenard and Prince 1992). I_{LHb} appears to possess permeation characteristics midway between those of the two thalamic LVA currents; its peak amplitude was essentially unaffected by Ba^{2+} substitution. The clear differences in relative current amplitude with Ba^{2+} or Ca^{2+} as the charge carrier could be due to differences in permeation through single channels or to effects on membrane screening charge (cf. Huguenard and Prince 1992). Single-channel recordings will be required to completely resolve this issue.

One prominent feature of I_{LHb} was its smaller peak amplitude compared with that of I_{VB} and I_{nRt}, measured using the same techniques in neurons from animals of the same ages. Although LHb cells were smaller than those of VB or nRt, the difference in size was not sufficient to account for the observed differences in current amplitude, which were still present when total capacitance was used to normalize for membrane area. The smaller current density may reflect a difference in either single-channel properties or the number of channels in the somata and proximal dendrites. In the current-clamp experiments of Wilcox et al. (1988), evidence was presented that the LVA channels, which were shown to have a critical role in determining the firing behavior of LHb neurons, may be abundant in dendrites—structures that were partially amputated by our isolation procedure. If LVA currents were preferentially localized in dendrites of LHb cells, compared with VB or nRt neurons, an apparent lower density would be observed in isolated LHb cells. Another possible explanation for the differences in LVA current density found in these experiments might be variations in ontogenetic development of T channels in neurons of different nuclei. This seems unlikely, however, because there was no correlation between I_{LHb} amplitude and age of the animal, indicating that I_{LHb} did not undergo significant ontogenic development between P6 and P34.

The finding that several characteristics of the I_{LHb} fell

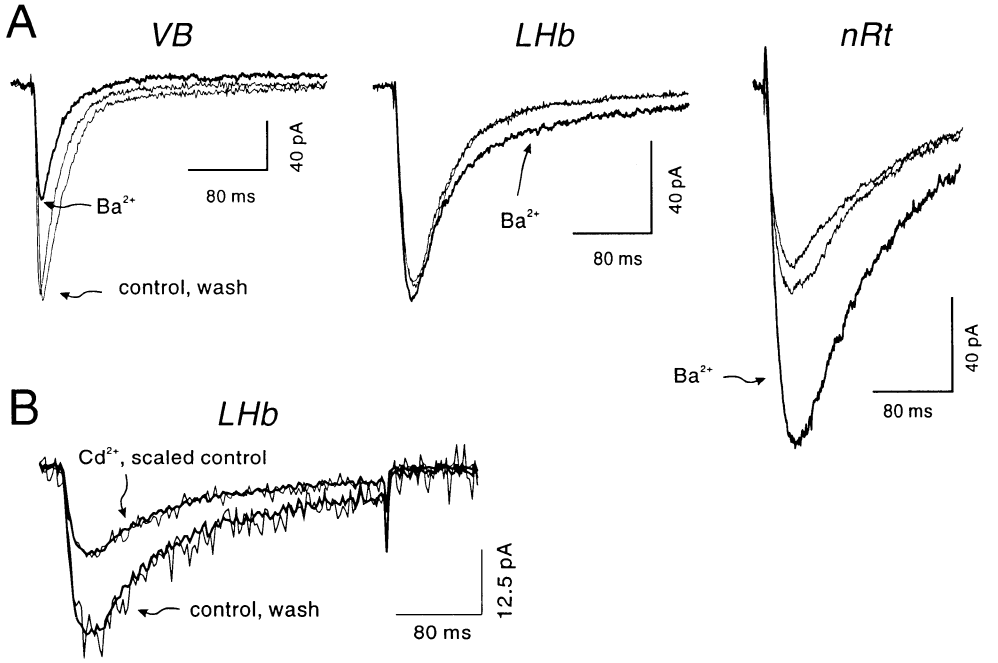

FIG. 7. Pharmacology of I_{LHb}. *A*: comparison of effects of Ba^{2+} substitution on LVA currents in LHb, VB, and nRt cells. Substitution of 3 mM Ba^{2+} for 3 mM Ca^{2+} reduces LVA at −40 mV in VB cells (*left*), increases it in nRt cells (*right*), but has little effect in I_{LHb} (*center*). For each cell type 3 traces are shown, including control, Ba^{2+} (dark lines) and wash. Each trace is average of 2–5 responses obtained in each situation. Note differences in calibration bars. *B*: reduction of I_{LHb} by 100 μM Cd^{2+}. Control trace (thick line) is average of 4 individual traces. I_{LHb} was reduced by ~45% (smaller current, thin line) by Cd^{2+}, and effect was reversible (thin, noisy wash trace). Control trace scaled down by 45% nearly exactly overlaps Cd^{2+} trace, indicating that early and late components are equally susceptible to blockade.

midway between those of I_{VB} and I_{nRt} raises the possibility that the inactivating Ca^{2+} current we studied here was not generated by a single channel type, but rather was due to a mixture of the two thalamic LVA channel types in single LHb neurons. Although this cannot be excluded without single-channel recordings, several lines of evidence argue against this explanation. First, the observed inactivation kinetics were not consistent with a mixture in which I_{VB}-type channels underlie fast inactivation and I_{nRt}-type channels underlie slow inactivation, because the time constant of the slow inactivation component of I_{LHb} was longer than the time constant of I_{nRt} inactivation. Second, because the steady-state inactivation curves for I_{nRt} and I_{VB} are slightly different (Huguenard and Prince 1992), a composite current would exhibit different inactivation kinetics depending on the conditioning potential, which would determine the relative contributions of I_{VB} and I_{nRt}. Therefore varying the prepulse amplitude would affect not only the peak current during the test pulse, but also the time course of the subsequent current decay. However, I_{LHb} decay rate was not so affected, because the steady-state inactivation curves measured 100 ms after current onset were the same as those measured at the current peak. Finally, the observation that I_{LHb} recovered from inactivation with the same slow time course as I_{nRt} is not consistent with a mixture of I_{VB} and I_{nRt}. A recently published computer model of the thalamic neuron (Huguenard and McCormick 1992; McCormick and Huguenard 1992) allowed us to simulate voltage-clamp experiments after specifying the characteristics of different conductances and their relative densities. We reasoned that were I_{LHb} to reflect a mixture of channel types, I_{nRt} would contribute the slow component of inactivation and I_{VB} would contribute the fast component. For our simulation we chose a 2:1 proportion of I_{VB}:I_{nRt}-type channels, because 33% was the highest percentage of *a2* (average 18%, Fig. 4*C*) in any given LHb cell at −40 mV, the potential at which recovery rate was measured, and this "best case" scenario would favor slow recovery (contributed by I_{nRt}). The *inset* in Fig. 6*A*, and filled squares in Fig. 6*B*, show that the simulation resulted in a time course of recovery from inactivation much different from that of I_{LHb}. The simulation data could be well fitted with a single exponential that had a time constant of 360 ms, which is quite close to the value experimentally measured for I_{VB} (300 ms; see Fig. 5*C*), but much faster than the 570 ms measured here for I_{LHb} and in a previous study for I_{nRt} (600 ms; Huguenard and Prince 1992).

The hypothesis underlying this study was that I_{LHb} would be the same as I_{nRt} because of similarities in rhythmogenic properties within nRt and LHb. The specific hypothesis is rejected, because I_{LHb} and I_{nRt} are different currents; nonetheless, the characteristics of the LVA current are presumably significant in determining firing and oscillatory characteristics within LHb. A feature common to both I_{nRt} and I_{LHb} is a slow and voltage-independent inactivation process that leads to prolonged Ca^{2+}-dependent low-threshold spikes and bursts. One consequence of the extended depolarization during such prolonged bursts would be increased activation of voltage- and Ca^{2+}-dependent currents, potentially leading to larger or more prolonged afterhyperpolarizations. These prominent transient hyperpolarizations would lead to rebound Ca^{2+}-dependent bursts and promote rhythmic burst generation. Because I_{LHb} did not turn out to be the same as I_{nRt}, then there must be other factors that promote rhythm generation in nRt and LHb cells. One obvious possibility would be cell-type–specific differences

in other ionic currents. For example, the existence of prominent Ca^{2+}-activated K^+ currents would promote large afterhyperpolarizations after each Ca^{2+}-dependent burst. If these hyperpolarizations were of sufficient amplitude and duration, they would promote rebound excitation through deinactivation of I_{LHb} (or I_{nRt}). Another possibility would be the presence of a hyperpolarization-activated cationic current, such as I_H in thalamic relay cells (McCormick and Pape 1990).

In summary, our data strongly suggest that, in addition to the two LVA currents already distinguished in thalamic nuclei, a third type is present in LHb cells. Although we cannot completely rule out the possibility that I_{LHb} is made up of a combination of two channel types, one similar to I_{VB} and the other similar to I_{nRt}, there are two arguments against that possibility. The first is that I_{LHb} shows uniform steady-state inactivation (Fig. 4*B*, ● vs. ⇑), and the second is that Cd^{2+} blocks early and late I_{LHb} to the same extent (Fig. 7*B*). Multiplicity of channel types has been well documented for HVA currents (Tsien et al. 1991), where molecular studies have permitted analysis of the differences in subunit assembly (reviewed by Catterall 1992) that can underlie differences in activation and inactivation properties. By analogy, we consider it likely that these three transient currents are part of a wider family of LVA channels that might result from either unique gene products or posttranslational changes. Additional members of this family might be present in other brain regions and contribute to the definition of unique firing properties and functional characteristics of particular types of neurons.

We thank E. Brooks and C. Pisaturo for technical assistance.

This work was supported by National Institute of Neurological Disorders and Stroke Grants NS-06477 and NS-12151 and by the Morris and Pimley Research Funds.

Address for reprint requests: J. R. Huguenard, Dept. of Neurology and Neurological Sciences, Rm. M016 Stanford University Medical Center, Stanford, CA 94305.

Received 17 December 1992; accepted in final form 5 March 1993.

REFERENCES

ALDRICH, R. W., COREY, D. P., AND STEVENS, C. F. A reinterpretation of mammalian sodium channel gating based on single channel recording. *Nature Lond.* 306: 436–441, 1983.

AVANZINI, G., DECURTIS, M., PANZICA, F., AND SPREAFICO, R. Intrinsic properties of nucleus reticularis thalami neurones of the rat studied in vitro. *J. Physiol. Lond.* 416: 111–122, 1989.

CARBONE, E. AND LUX, H. D. Kinetics and selectivity of a low-voltage-activated calcium current in chick and rat sensory neurones. *J. Physiol. Lond.* 386: 547–570, 1987.

CATTERALL, W. A. Functional subunit structure of voltage-gated calcium channels. *Science Wash. DC* 253: 1499–500, 1991.

CHEN, C. AND HESS, P. Mechanism of gating of T-type calcium channels. *J. Gen. Physiol.* 96: 603–630, 1990.

COULTER, D. A., HUGUENARD, J. R., AND PRINCE, D. A. Calcium currents in rat thalamocortical relay neurones: kinetic properties of the transient, low-threshold current. *J. Physiol. Lond.* 414: 587–604, 1989.

COULTER, D. A., HUGUENARD, J. R., AND PRINCE, D. A. Differential effects of petit mal anticonvulsants and convulsants on thalamic neurones: calcium current reduction. *Br. J. Pharmacol.* 100: 80–806, 1990.

FORSCHER, P. AND OXFORD, G. S. Modulation of calcium channels by norepinephrine in internally dialyzed avian sensory neurons. *J. Gen. Physiol.* 85: 743–763, 1985.

FOX, A. P., NOWYCKY, M. C., AND TSIEN, R. W. Kinetic and pharmacological properties distinguishing three types of calcium currents in chick sensory neurons. *J. Physiol. Lond.* 394: 149–172, 1987.

HAMILL, O. P., MARTY, A., NEHER, E., SAKMANN, B., AND SIGWORTH, F. J. Improved patch-clamp techniques for high-resolution current recording from cells and cell-free membrane patches. *Pfluegers Arch.* 391: 85–100, 1981.

HODGKIN, A. L. AND HUXLEY, A. F. A quantitative description of membrane current and its application to conduction and excitation in nerve. *J. Physiol. Lond.* 117: 500–544, 1952.

HUGUENARD, J. R., GUTNICK, M. J., AND PRINCE, D. A. Further diversity of LVA Ca channels within burst firing neurons of the CNS: long lasting currents in rat lateral habenular cells. *Soc. Neurosci. Abstr.* 18: 431, 1992.

HUGUENARD, J. R. AND MCCORMICK, D. A. Simulation of the currents involved in rhythmic oscillations in thalamic relay neurons. *J. Neurophysiol.* 68: 1373–1383, 1992.

HUGUENARD, J. R. AND PRINCE, D. A. A novel T-type current underlies prolonged Ca^{2+}-dependent burst firing in GABAergic neurons of rat thalamic reticular nucleus. *J. Neurosci.* 12: 3804–3817, 1992.

JONES, E. G. *The Thalamus.* New York: Plenum, 1985.

KAY, A. R. AND WONG, R. K. S. Isolation of neurons suitable for patch-clamping from adult mammalian central nervous systems. *J. Neurosci. Methods* 16: 227–238, 1986.

LERESCHE, N., JASSIK-GERSCHENFELD, D., HABY, M., SOLTESZ, I., AND CRUNELLI, V. Pacemaker-like and other types of spontaneous oscillations of thalamocortical cells. *Neurosci. Lett.* 113: 72–77, 1990.

LLINÁS, R. R. AND GEIJO-BARRIENTOS, E. In vitro studies of mammalian thalamic and reticularis thalami neurons. In: *Cellular Thalamic Mechanisms,* edited by M. Bentivoglio and R. Spreafico. Amsterdam: Excerpta Medica, 1988, p. 23–33.

MCCORMICK, D. A. AND HUGUENARD, J. R. A model of the electrophysiological properties of thalamocortical relay neurons. *J. Neurophysiol.* 68: 1384–1400, 1992.

MCCORMICK, D. A. AND PAPE, H.-C. Properties of a hyperpolarization-activated cation current and ins role in rhythmic oscillations in thalamic relay neurons. *J. Physiol. Lond.* 431: 291–318, 1990.

MCCORMICK, D. A. AND WANG, Z. Serotonin and noradrenaline excite GABAergic neurones of the guinea-pig and cat nucleus reticularis thalami. *J. Physiol. Lond.* 442: 235–255, 1991.

MULLE, C., MADARIAGA, A., AND DESCHÊNES, M. Morphology and electrophysiological properties of reticularis thalami neurons in cat: in vivo study of a thalamic pacemaker. *J. Neurosci.* 6: 2134–2145, 1986.

MULLE, C., STERIADE, M., AND DESCHÊNES, M. Absence of spindle oscillation in the cat anterior thalamic nuclei. *Brain Res.* 334: 2169–171, 1985.

PAPE, H.-C. AND MCCORMICK, D. A. Noradrenaline and serotonin selectively modulate thalamic burst firing by enhancing a hyperpolarization-activated cation current. *Nature Lond.* 340: 715–718, 1989.

STERIADE, M., DESCHÊNES, M., DOMICH, L., AND MULLE, C. Abolition of spindle oscillations in thalamic neurons disconnected from nucleus reticularis thalami. *J. Neurophysiol.* 54: 1473–1497, 1985.

STERIADE, M., DOMICH, L., OAKSON, G., AND DESCHÊNES, M. The deafferented reticular thalamic nucleus generates spindle rhythmicity. *J. Neurophysiol.* 57: 260–273, 1987.

SWANDULLA, D., CARBONE, E., AND LUX, H. D. Do calcium channel classifications account for neuronal calcium channel diversity? *Trends Neurosci.* 14: 46–51, 1991.

TANG, C.-M., PRESSER, F., AND MORAD, M. Amiloride selectively blocks the low threshold (T) calcium channel. *Science Wash. DC* 240: 213–215, 1988.

TSIEN, R. W., ELLINOR, P. T., AND HORNE, W. A. Molecular diversity of voltage-dependent Ca^{2+} channels. *Trends Pharmacol. Sci.* 12: 349–354, 1991.

WILCOX, K. S., GUTNICK, M. J., AND CHRISTOPH, G. R. Electrophysiological properties of neurons in the lateral habenula nucleus: an in vitro study. *J. Neurophysiol.* 59: 212–225, 1988.